ISCAS 2000 - IEEE International Symposium on Circuits and Systems, May 28-31, 2000, Geneva, Switzerland

A REAL FREQUENCY TECHNIQUE OPTIMIZING BROADBAND EQUALIZER ELEMENTS

Thomas R. Cuthbert, Jr., Ph.D.

Greenwood, Arkansas 72936, USA
trcpep@aol.com

ABSTRACT

A practical real frequency technique for broadband impedance matching is based on bilinear reflection behavior versus lumped and distributed element variables. An efficient grid search locates a likely-global solution so that a precise constrained gradient optimization can eliminate unnecessary elements in candidate networks.

1. INTRODUCTION

Broadband matching requires a lossless two-port matching network (equalizer) to minimize the maximum loss at passband frequencies. Usually the load and/or source are not pure resistances. See Figure 1; the maximum available source power is $P_{as}=|E_S|^2/4R_S$, where $Z_S \equiv R_S+jX_S$. The relative power delivered to the load, Z_L, at a given frequency is

$$T \equiv \frac{P_L}{P_{aS}} = 1 - \left|\rho_{in}\right|^2 . \qquad (1)$$

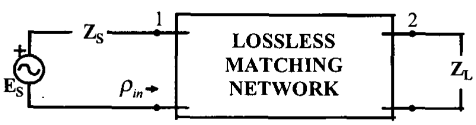

Figure 1. Broadband matching network terminations.

The generalized reflection coefficient is

$$\rho_{in} \equiv \frac{Z_{in} - Z_S^*}{Z_{in} + Z_S} . \qquad (2)$$

Reflectance is reflection magnitude at a given frequency and is constant at all two-port interfaces because of conservation of power. The minimax objective in broadband matching is

$$\underset{x}{Min} \left[f(x, \omega) \equiv \underset{\omega}{Max} \left|\rho(x, \omega)\right| \right], \quad x \in R^n , \ \omega_1 \le \omega \le \omega_m ; \qquad (3)$$

n is the number of degrees of freedom in the equalizer, i.e., the element values, and m passband frequencies are selected.

Two broadband matching techniques are classical insertion loss theory and real frequency techniques (RFT) [1]. The former is applicable to very few practical matching problems. The RFT is a numerical optimization method that is applicable to a wide range of practical problems, and utilizes frequency-sampled load and/or source impedance data. Numerical optimization adjusts free parameters (variables) to minimize an objective function, e.g. least squares [2] or random search [3]. A well-known RFT employs one or more approximation and optimization stages and ends with polynomial synthesis [1]. The variables are polynomial coefficients or s-plane root coordinates, so parts of that process are extremely ill-conditioned [6].

This paper describes a well-conditioned RFT with an optimization objective that depends on variables in simple ways, leading to likely-global optimal results. The variables are values of equalizer elements, which may be mixed lumped and distributed. This new technique avoids linear, nonlinear, or rational approximations and polynomial synthesis. An optimal equalizer topology is not known in advance; otherwise, some common optimization algorithms might find optimal solutions. Here a useful candidate equalizer topology is selected, and the grid approach to broadband impedance matching (GRABIM) automatically eliminates all unnecessary elements. The theory is discussed, the two optimization stages are described, a well known example is solved, and references are provided.

2. REFLECTION CHARACTERISTICS

The GRABIM technique utilizes a candidate equalizer topology with vector $x=[x_j]$ containing all the variable element values and operates on the reflectance at each passband frequency versus each element value, x_j, j=1...n. Choose m≈2n passband frequencies, ω_i, i=1...m, each associated with data constants for R_S, X_S, R_L, and X_L. The generalized Smith chart in Figure 2 illustrates how reflectance at a frequency varies with a series reactance through all positive and negative values, typical of the intrinsic *bilinear* behavior of each series (parallel) branch reactance (susceptance).

Figure 3 shows Thevenin interfaces for each kind of equalizer element, noting that reflectance is constant throughout the equalizer at a given frequency. Subnetworks N_1 and N_2 might be an L, C, LC pair (*trap*) or transmission-line open- or short-circuit stub. Subnetworks N_1, N_2, and N_3 each produce at most a *unimodal* (single minimum) reflectance skewed by the nonlinear dependence of angle ϕ on L, C, t, or stub Z_0 and θ variables, the last potentially periodic. Cascade transmission line (CASTL) length, θ, produces a circular locus strictly within the interior of a generalized Smith chart, and the CASTL characteristic impedance, Z_0, produces a reflectance that is at most *bimodal* (two minima). These slight variations from unimodality are easily avoided by the grid search described in Section 3.

0-7803-5482-6/99/$10.00 ©2000 IEEE

Authorized licensed use limited to: UNIVERSIDAD CARLOS III MADRID. Downloaded on February 17,2022 at 14:07:26 UTC from IEEE Xplore. Restrictions apply.

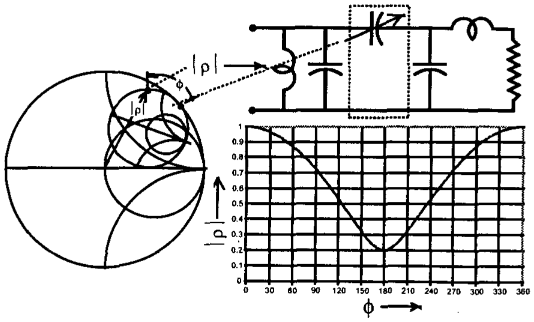

Figure 2. Origin of reflectance curves versus variable.

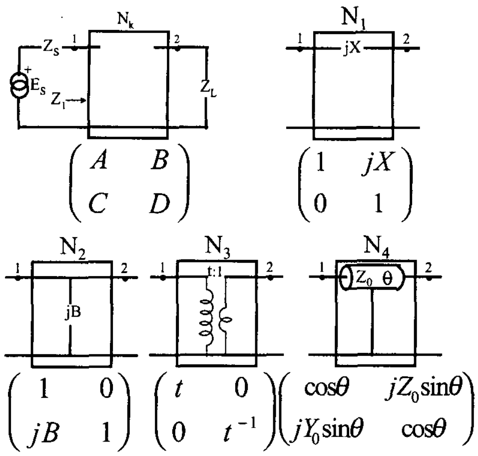

Figure 3. Interfaces for lossless subnetworks.

Typical reflectance cross sections versus a series inductance are shown in Figure 4. The curves at each frequency are similar to segments of the ϕ curve in Figure 2 except for the skewing in the abscissa. The *envelope* is defined to be the worst-case reflectance and is composed of piecewise arcs; the derivative of the envelope is discontinuous where the arc segments join. Broadband matching problem (3) is solved by finding the element values in vector x for the common minima on their respective envelopes and varying that x to obtain the lowest-possible minimum reflectance. Further consideration of Figure 4 shows that additional passband frequency samples would interpolate between reflectance curves at adjacent frequencies and only more precisely define the envelope, so choice of samples is not critical.

It is important to observe the reflectance curves for $\omega = 0.4$, 0.5, and 0.6 rad/s in Figure 4. They are still just segments of the ϕ curve in Figure 2, and it is not unusual for all sample frequencies to produce a *monotonic* (no minimum) envelope as opposed to a unimodal envelope for certain element variables. If only those three particular frequencies in Figure 4 are considered, the series branch would be unnecessary and would be removed (L=0) under the condition that no other elements were changed.

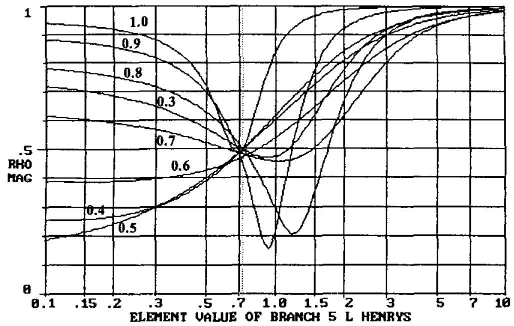

Figure 4. Typical reflectances versus a series branch inductance. Each normalized frequency curve is a skewed segment of the curve in Figure 2.

3. DIRECT SEARCH

The precise search described in Section 4 removes all unnecessary elements but must be started from an approximate solution to (3). Also, there may be many local minima of (3), especially when unnecessary elements are present. Classical insertion loss theory and other broadband techniques indicate that each element in vector x will be in the range $1/25 \le x_j \le 25$ for sampled data and equalizers normalized to one ohm and one rad/s. Normalized L, C, t, and Z_0 values are explored within that range; only one L or C is varied in traps, the other C or L being dependent on a fixed null frequency. Well-scaled mapping functions are used to relate transmission line lengths to the x_j range, which is in turn mapped to log space; see Figure 4.

A typical nonsmooth surface at one frequency for two of many variables is shown in Figure 5; all sections resemble Figure 4. An efficient direct search technique for locating the global

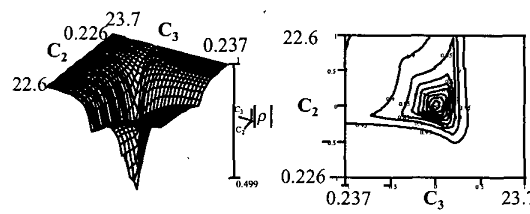

Figure 5. A typical envelope surface for two variables.

minimum is to evaluate the envelope surface at a pattern of points in variable log space. Figure 6 shows such a pattern, which can be considered an archeological grid over the terrain in Figure 5. During a search iteration, each grid point defines a set of element values, and the worst reflectance over all frequency samples determines the envelope surface value. Some point in the pattern will have the least worst-case reflectance, so the pattern is recentered on that point for another iteration.

When a better point cannot be found, the pattern *granularity* (point spacing) is reduced by factor 4, and the search is restarted. A noncritical choice is to center the initial grid on unity; then only three reductions in granularity are required, a total factor of 1/64. The number of pattern trial points is decreased as the

Authorized licensed use limited to: UNIVERSIDAD CARLOS III MADRID. Downloaded on February 17,2022 at 14:07:26 UTC from IEEE Xplore. Restrictions apply.

number of equalizer elements increases from 2 to 10 so that about 1000 envelope surface evaluations are required for each iteration. Also, there are many programming strategies for improving search efficiency.

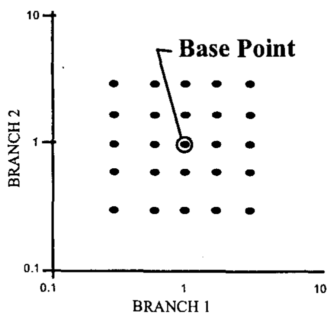

Figure 6. A 5×5 lattice (grid) for two variables.

It has been shown that this grid search converges unfailingly to a point where the surface is nondifferentiable or the gradient is zero [4]. This grid search in log space also avoids local minima that sometimes occur in coordinate sections related to transmission-line variables and avoids the local minima that are usually observed on the principal diagonals of the pattern hypercube in n space. Examination of cross sections and diagonals for many realistic matching data sets and topologies has shown it reasonable to expect the reflectance envelope minimum found to be global.

4. CONSTRAINED GRADIENT OPTIMIZATION

The broadband matching objective in (3) is nonsmooth with discontinuous derivatives. Generally, direct searches do not require derivatives to exist, but are known to have very slow final convergence. However, gradient search based on first partial derivatives usually converges rapidly to a nearby minimum. Therefore, (3) is converted to an equivalent differentiable optimization problem by adding one more variable, x_{n+1}, to the x vector:

$$\underset{x}{Min}\; x_{n+1} \text{ subject to } \left|\rho\left(x, \omega_i\right)\right| \le x_{n+1},\; i = 1 \quad m. \quad (4)$$

This objective function is linear, and the m inequality reflectance constraints are differentiable functions.

The envelope minimum in Figure 4 is enlarged in Figure 7. It is seen that x_{n+1} has been reduced to 0.50 with the variable for the inductance having the value 0.72. Also, this solution is determined by binding constraints at 0.3, 0.4, 0.5, 0.8, and 1.0 rad/s; the remaining three constraints are not binding. The standard constrained optimization problem in (4) can be solved by several methods. The Lagrange multiplier method is a precise and rapidly convergent gradient algorithm that is reliable when started near a minimum [2]; it replaces (4) with

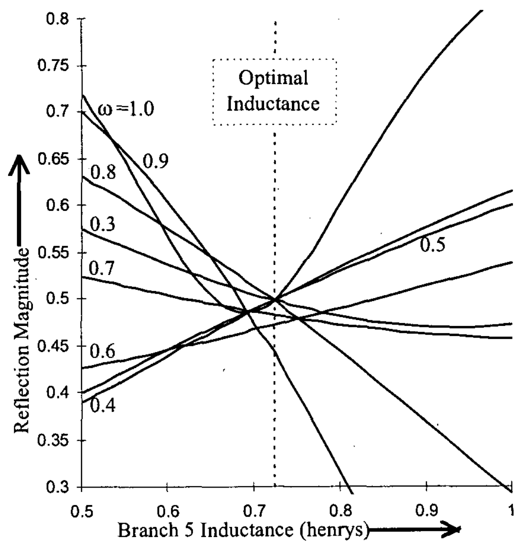

Figure 7. Details of binding reflectances in Figure 4.

$$\underset{x}{Min}\; x_{n+1} + \sum_{i=1}^{m} s_i \max\left[\left|\rho\left(x, \omega_i\right)\right| - x_{n+1} + u_i, 0\right]^2. \quad (5)$$

The formulation in (5) introduces m pairs of weights, s_i, and offsets, u_i. The u_i offset the origins of the constraints so that the s_i weights need not become infinite as with ordinary penalty function optimizers [2].

A particularly simple Lagrange multiplier algorithm [5] starts with the x vector from the grid search and x_{n+1} set to the maximum reflectance, all s_i=1, and all u_i=0. There are two loops: The outer loop adjusts the s_i and u_i based on how the worst-case binding constraint increased or decreased. The inner loop obtains the minimum in (5) with fixed values of s_i and u_i; first derivatives are continuous. The inner loop is an unconstrained minimization except for element bounds or holds, requires first partial derivatives, and converges at a quadratic rate. The outer loop is an approximate minimizer that converges at a linear rate [2]. The minimum reflectance is obtained subject to the binding constraints within a few iterations; see Figure 7. Significantly, the m $\cdot s_i \times u_i$ products at the constrained minimum are equal to the Lagrange multipliers associated with (4); that is one basis for adjusting the s_i and u_i values in the outer loop. The gradient search is also conducted in variable log space, which guarantees positive element values and normalizes the derivatives for optimal scaling.

The grid search requires several thousand evaluations of reflectance, and the Lagrange multiplier method requires reflectances and their first partial derivatives with respect to each component of x. Fortunately, these values can be obtained exactly with great efficiency using the element ABCD parameters in Figure 3 [6]. A special advantage of GRABIM is that the overall equalizer ABCD parameters at each frequency need be computed only once. Therefore, sets of Z_L and Z_S data defining

Authorized licensed use limited to: UNIVERSIDAD CARLOS III MADRID. Downloaded on February 17,2022 at 14:07:26 UTC from IEEE Xplore. Restrictions apply.

neighborhoods of uncertain impedance at each frequency also can be broadband matched efficiently.

5. EXAMPLE

There is a double-match example that cannot be solved by the classical insertion loss method [7]. The source and load models shown in Figure 8 are seldom known; however, their impedance data in the desired passband from 0.3 to 1.0 rad/s in 0.1 intervals are assumed given. The source resistance being zero at 1.29 rad/s is particularly difficult. The RFT method in [7] utilizes several arbitrary approximations, optimizations, and synthesis steps to yield a six-element equalizer with passband loss 0.85 to 1.42 dB.

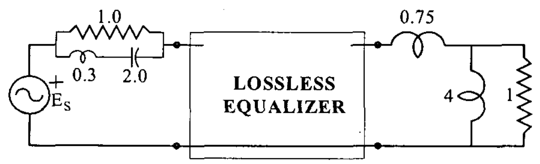

Figure 8. A difficult broadband matching problem.

The GRABIM technique used the same data and a six- element equalizer topology consisting of a Pi of L's at the source followed by a Pi of C's at the load. (The source is capacitive and the load is inductive; Pi networks implicitly contain ideal transformers.) The grid search required 7026 network analyses performed in 2 seconds by a 200 MHz PC; the worst-case insertion loss was reduced to 2.6 dB. A few Lagrange multiplier loops reduced the loss to 1.24 dB while automatically removing one L and one C. See Figure 9(a); two other solutions started from other topologies also are shown in Figures 9(b) and 9(c).

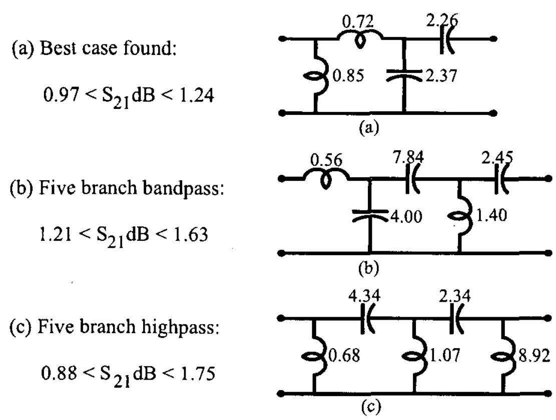

Figure 9. Three full-rank broadband network solutions.

6. SUMMARY

The GRABIM RFT is a pure numerical optimization algorithm that is fast, simple, and reliable. It solves double-match problems as easily as single-match problems. GRABIM locates a likely-global optimal solution for a given topology and eliminates unnecessary branches during a two-stage process of optimizing equalizer elements. Mixed lumped and distributed elements are allowed, based on clearly defined behavior of reflection magnitude versus element variables. Inexpensive, documented software is available from the author.

GRABIM features:

- Measured single- or double-match source and load impedance data at sampled passband frequencies,
- Noncritical choice of frequency samples,
- Mixed lumped/distributed equalizer elements,
- Bandpass or lowpass equalizers,
- Arbitrary or stored candidate topologies of varying degree,
- Automatic elimination of unnecessary elements,
- No element initial values required,
- Bounds or holds on element values,
- Efficient broadband matching of impedance neighborhoods,
- Likely-global optimal solutions, and
- Proven, well-conditioned numerical techniques.

7. REFERENCES

[1] Carlin, H. J. and P. P. Civalleri (1998). *Wideband Circuit Design.* NY: CRC Press.

[2] Fletcher, R. (1980-1981). *Practical Methods of Optimization: Unconstrained Optimization*, Vol. 1, and *Constrained Optimization*, Vol. 2. NY: John Wiley.

[3] Dedieu, H., C. Dehollain, J. Neirynck, and G. Rhodes (1994). A new method for solving broadband matching problems. *IEEE Trans. Circuits and Sys.*, V41, N9. Sept.:561-571.

[4] Torczon, V. (1991). On the convergence of the multidirectional search algorithm. *SIAM J. Opti.*, V1, N1. Feb.:123-145.

[5] Powell, M. J. D. (1969). A method for nonlinear constraints in minimization problems, in *Optimization*, R. Fletcher, Ed. NY: Academic Press, pp. 283-297.

[6] Orchard, H. J. (1985). Filter design by iterated analysis. *IEEE Trans. Circuits & Sys.*, V32, N11. Nov.:1089-96.

[7] Yarman, B. S. and A. Fettweis (1990). Computer-aided double matching via parametric representation of Brune functions. *IEEE Trans. Circuits & Sys.*, V37, N2. Feb.:212-222.

Authorized licensed use limited to: UNIVERSIDAD CARLOS III MADRID. Downloaded on February 17,2022 at 14:07:26 UTC from IEEE Xplore. Restrictions apply.